Proceedings of the 2009 IEEE International Conference on Systems, Man, and Cybernetics
San Antonio, TX, USA - October 2009

Networked Predictive Control of Magnetic Levitation System

Bo Wang
School of Engineering
University of Warwick
Coventry, CV4 7AL, UK
b.wang@warwick.ac.uk

Guo-Ping Liu and David Rees
Faculty of Advanced Technology
University of Glamorgan
Pontypridd, CF37 1DL, UK
gpliu@glam.ac.uk, drees@glam.ac.uk

***Abstract*—This paper discusses the control of a magnetic levitation (MagLev) system over networks. In order to improve the control performance, the networked predictive control method is employed based on the feedback linearization and direct local linearization models of the nonlinear MagLev system. Further a test-rig is set up to implement the above control. Simulation and experiment results show that the networked predictive control has clear performance advantages over other networked control strategies which do not incorporate compensation for the network-induced delay.**

***Index Terms*—Networked predictive control, Magnetic levitation system, Feedback linearization, NetCon embedded system.**

I. Introduction

Magnetic levitation (MagLev) system has been widely studied and applied to high-speed transportation, magnetic bearing, vibration isolation and so on [1], [2], [3], [4], [5], due to its advantage of frictionless contact.

Magnetic levitation system is typically open-loop unstable, time-varying and highly nonlinear, so it presents significant control challenges. Generally, most control methods are based on a linearized model of the MagLev system at a nominal operating point [1], [6]. The tracking performance of the resulting closed-loop system, however, deteriorates rapidly with increasing deviations from the nominal operating point. Two main approaches to improve the tracking performance have been reported in the literature. One is that of gain scheduling where the nonlinearity of the MagLev system is successively linearized at various operating points with a suitable controller designed for each of these operating points. Gain scheduling controllers [7] require the operating range to be broken up into very fine intervals and stored in a look-up table of controller gains. The other approach is feedback linearization [6], [8], [9], [10], [11], which utilizes the nonlinear description of the system and hence yields consistent performance largely independent of operating points. Other control methods, like sliding mode control [12], back-stepping control [13] and dynamic surface control [14], were also proposed to actively tackle system uncertainties and robustness. As for the issue of the model identification of MagLev system, some results can be found in [15], [16].

Control of a MagLev system over networks presents another level of challenge. Network-induced transmission delay and data dropout in the closed-loop make it more difficult for the system to achieve the desired performance, even to stabilize the system is a particular challenge. Because MagLev system is a fast dynamic system, practical control of it generally requires a small sampling period. This means the resulting network-induced delay might be large w.r.t. the sampling period. Networked control of MagLev system over a LAN has been reported in [17], [18], where an auto-regressive prediction model is built to compensate for the network-induced delay.

Recently networked predictive control (NPC) method [19], [20], [21] has been developed to actively and efficiently compensate the delay and data dropout. In this paper, several control methods based on the local linearization model and feedback linearization model of the plant and their networked predictive control versions are studied for a MagLev prototype system. In order to implement these control strategies, a MagLev test-rig including MagLev system, data acquisition and networked controller is set up.

II. Modeling of MagLev system

The MagLev system studied in this paper was manufactured by BYTRONIC Ltd [22], which mainly consists of power interface, electro-magnet, hollow steel ball, ball position sensor and coil current sensor. Its schematic diagram is shown in Figure 1. The basic principle of this system is to apply a voltage to the electro-magnet to generate magnet force and then to keep the ball levitated. The ball position (air gap from electro-magnet to ball) is measured by a photoelectric sensor which detects the photo level received from a photo emitter. The photo level which the ball (in the middle of detector and emitter) allows to go through reflects its position. The power interface between the supplied power and the power applied to the electro-magnet is governed by a PWM signal which is from, for example, the controller. The power interface also senses the coil current passing through the electro-magnet.

According to fundamental principles of dynamics [6], [11], the MagLev system shown in Figure 1 satisfies

$$\begin{aligned} \dot{y}(t) &= v(t) \\ m\dot{v}(t) &= mg - F(i,y) \\ L(y)\dot{i}(t) &= E(t) - Ri(t) \end{aligned} \tag{1}$$

978-1-4244-2794-9/09/$25.00 ©2009 IEEE

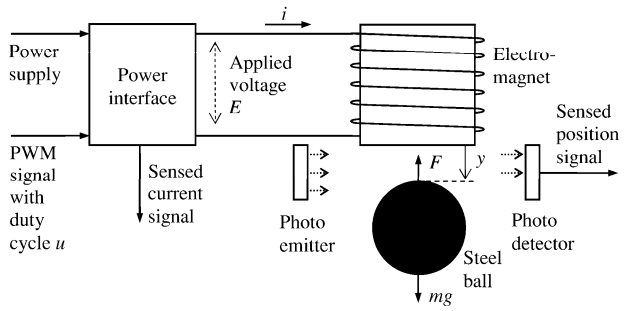

Figure 1. Schematic diagram of BYTRONIC MagLev system

where $y(t)$ is the ball position, $v(t)$ is the ball velocity, $i(t)$ is the coil current, $E(t)$ is the applied voltage, $F(t)$ is the electromagnetic force, $L(y)$ is the coil inductance, m is the ball mass, g is the gravity acceleration, and R is the coil resistance. Note that $F(i,y)$ is nonlinear w.r.t. $i(t)$ and $y(t)$, so is $L(y)$ w.r.t. $y(t)$.

In this MagLev system, nonlinearity characteristics in F and L are respectively described in [22] by

$$F(i,y) = i(t)^2 \frac{F_{emP1}}{F_{emP2}} e^{-\frac{y(t)}{F_{emP2}}} \quad (2)$$

$$L(y) = R\frac{f_{iP1}}{f_{iP2}} e^{-\frac{y(t)}{f_{iP2}}}. \quad (3)$$

Furthermore, the relation of the applied voltage E and the duty cycle u of the PWM signal is explicitly expressed as

$$\frac{E(t)}{R} = k_i u(t) + c_i. \quad (4)$$

Clearly, u is in the interval $[0,1]$. In equations (2), (3) and (4), F_{emP1}, F_{emP2}, f_{iP1}, f_{iP2}, c_i and k_i are parameters determined by the characteristics of the coil, magnetic core and the ball. These parameters as well as m and g as shown in Table I are given in [22]. Note that some of the above parameters might not be accurate because of possible changes in the physical properties of the system. Replacing corresponding items in (1) with (2), (3) and (4), the system model is converted to an affine nonlinear state-space model

$$\begin{aligned} \dot{x}_1(t) &= x_2(t) \\ \dot{x}_2(t) &= -\frac{1}{m}\frac{F_{emP1}}{F_{emP2}} e^{-\frac{x_1(t)}{F_{emP2}}} x_3(t)^2 + g \\ \dot{x}_3(t) &= \frac{f_{iP2}}{f_{iP1}} e^{\frac{x_1(t)}{f_{iP2}}} (k_i u(t) + c_i - x_3(t)) \end{aligned} \quad (5)$$

where $x = [x_1\ x_2\ x_3]^T$ is the system state with $x_1 = y$, $x_2 = v$ and $x_3 = i$, and u is the input.

III. Networked feedback linearization predictive control

The design of networked control of the MagLev system is concerned with two aspects. One is the nonlinearity feature of the process, and the other is the network-induced delay. For the former, control methods based on feedback linearization model and local linearization model of (5) are discussed. For the latter, a networked predictive control strategy is applied.

Table I
Parameters of BYTRONIC MagLev system.

Parameters	Values	Units
m	5.7×10^{-2}	[kg]
g	9.81	[m/s^2]
F_{emP1}	1.75×10^{-2}	[H]
F_{emP2}	5.82×10^{-3}	[m]
f_{iP1}	1.41×10^{-4}	[m·s]
f_{iP2}	4.56×10^{-3}	[m]
c_i	2.43×10^{-2}	[A]
k_i	2.52	[A]

The network-induced delay $\tau(t)$ is the round-trip delay which includes sensor-to-controller delay $\tau_{sc}(t)$ and controller-to-actuator delay $\tau_{ca}(t)$. Their discrete-time versions w.r.t. the sampling period are denoted as $\tau(k)$, $\tau_{sc}(k)$ and $\tau_{ca}(k)$, respectively. $\tau(k)$ is assumed to have an upper-bound $\bar{\tau}$.

In this MagLev system, ball position and coil current are both measured. Ball velocity can be approximately obtained by numerically differentiating the position signal at sampling instants, i.e.,

$$x_2(k) = \frac{x_1(k) - x_1(k-1)}{h}$$

where h is the sampling period. Thus, the system has full state feedback.

A. Feedback linearization

In model (5), using the following nonlinear transformation coordinates reported by [23], [24], [25]

$$\begin{aligned} x_{fl1}(t) &= x_1(t) \\ x_{fl2}(t) &= x_2(t) \\ x_{fl3}(t) &= -\frac{1}{m}\frac{F_{emP1}}{F_{emP2}} e^{-\frac{x_1(t)}{F_{emP2}}} x_3(t)^2 + g. \end{aligned} \quad (6)$$

Note that the state x_{fl3} stands for the ball acceleration. In the new coordinates, the system model changes to

$$\begin{aligned} \dot{x}_{fl1}(t) &= x_{fl2}(t) \\ \dot{x}_{fl2}(t) &= x_{fl3}(t) \\ \dot{x}_{fl3}(t) &= \alpha(x(t)) + \beta(x(t))u(t) \end{aligned} \quad (7)$$

where

$$\begin{aligned} \alpha(x(t)) = &\frac{1}{m}\frac{F_{emP1}}{F_{emP2}^2} e^{-\frac{x_1(t)}{F_{emP2}}} x_2(t) x_3(t)^2 \\ &-\frac{2}{m}\frac{F_{emP1}}{F_{emP2}}\frac{f_{iP2}}{f_{iP1}} e^{\frac{x_1(t)}{f_{iP2}} - \frac{x_1(t)}{F_{emP2}}} x_3(t) \times \\ &(c_i - x_3(t)) \end{aligned} \quad (8)$$

$$\beta(x(t)) = -\frac{2k_i}{m}\frac{F_{emP1}}{F_{emP2}}\frac{f_{iP2}}{f_{iP1}} e^{\frac{x_1(t)}{f_{iP2}} - \frac{x_1(t)}{F_{emP2}}} x_3(t). \quad (9)$$

In (7), if $u(t)$ is designed as

$$u(t) = \frac{-\alpha(x(t)) + u_{fl}(t)}{\beta(x(t))}, \quad (10)$$

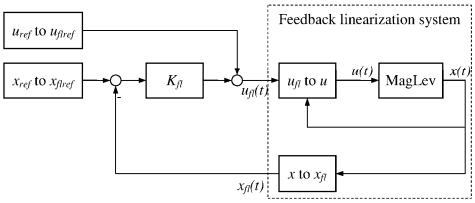

Figure 2. Feedback linearization control system structure without inclusion of the network.

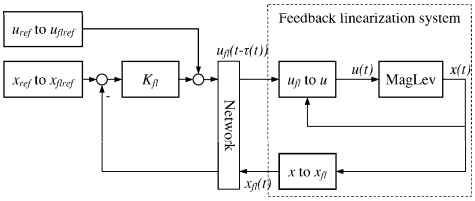

Figure 3. Feedback linearization control system structure with network.

then the resulting system becomes linear, so that

$$\dot{x}_{fl}(t) = A_{fl}x_{fl}(t) + B_{fl}u_{fl}(t) \tag{11}$$

with

$$A_{fl} = \begin{bmatrix} 0 & 1 & 0 \\ 0 & 0 & 1 \\ 0 & 0 & 0 \end{bmatrix}, B_{fl} = \begin{bmatrix} 0 \\ 0 \\ 1 \end{bmatrix}.$$

Note that (10) is feasible because $x_3(t)$ (coil current $i(t)$) is greater than 0. Clearly, feedback linearization model (11) is controllable, so that

$$u_{fl}(t) = K_{fl}\left(x_{flref} - x_{fl}(t)\right) + u_{flref}. \tag{12}$$

When considering local control (without network), static state-feedback control K_{fl} can be designed using many existing methods, such as pole-placement, optimization, etc. In (12), x_{flref} and u_{flref} are references which correspond to x_{ref} and u_{ref} and can be obtained from (6) and (8), (9) and (10), respectively. Figure 2 shows the system control structure after the above feedback linearization.

B. Networked feedback linearization predictive control

When considering networked control, as shown in Figure 3, the resulted feedback linearization system becomes

$$\dot{x}_{fl}(t) = A_{fl}x_{fl}(t) + B_{fl}u_{fl}(t - \tau(t)). \tag{13}$$

Note that in Figure 3, calculating the two blocks "u_{fl} to u" and "x to x_{fl}" is needed on the plant side. This is not a problem for a "smart" actuator or sensor. For (13), control gain K_{fl} in (12) should be designed to tolerate $\tau(t)$. Many literature addresses this issue in NCS, for example [26], [27], [28]. Here, in order to actively compensate for the network-induced delay, networked predictive method [19] is adopted. Firstly, sampling (11) with sampling period h gives

$$x_{fl}(k+1) = \Phi_{fl}x_{fl}(k) + \Gamma_{fl}u_{fl}(k), \tag{14}$$

where $\Phi_{fl} = e^{A_{fl}h}$ and $\Gamma_{fl} = \int_0^h e^{A_{fl}\eta}d\eta B_{fl}$. Then, at the controller side, denote the received state as $z(k)$, which is the delay version of $x_{fl}(k)$, i.e., $z(k) = x_{fl}(k - \tau_{sc}(k))$. Then, according to a feedback gain K_{fl} and system model Φ_{fl} and Γ_{fl}, the control prediction sequence up to the maximum round-trip delay $\bar{\tau}$ is

$$V(k) = \begin{bmatrix} v(k|k) \\ v(k+1|k) \\ \vdots \\ v(k+\bar{\tau}|k) \end{bmatrix}$$

which is obtained on the controller side by recursively calculating the following two equations [21]

$$\begin{cases} z(k+i+1|k) & = \Phi_{fl}z(k+i|k) + \Gamma_{fl}v(k+i|k) \\ & i = 0, 1, \cdots, \bar{\tau} - 1 \\ v(k+i|k) & = K_{fl}\left(x_{flref} - z(k+i|k)\right) + u_{flref} \\ & i = 0, 1, \cdots, \bar{\tau} \end{cases}. \tag{15}$$

The whole prediction sequence $V(k)$ is sent back to the controller side as

$$V(k - \tau_{ca}(k)) = \begin{bmatrix} v(k-\tau(k)|k-\tau(k)) \\ v(k-\tau(k)+1|k-\tau(k)) \\ \vdots \\ v(k-\bar{\tau}|k-\tau(k)) \end{bmatrix}.$$

Then according to the actual measured round-trip delay $\tau(k)$, the proper element $v(k|k-\tau(k))$ is chosen as the control input, i.e. $u_{fl}(t) = v(k|k-\tau(k))$. Thus delay $\tau(k)$ is compensated. NPC method can similarly deal with the data dropout in network and its stability analysis is considered in [20].

IV. Networked direct linearization predictive control

Given an operating point $x_0 = [x_{10}, x_{20}, x_{30}]^T$ and u_0, model (5) is linearized as

$$\dot{x}(t) = A_{dl}x(t) + B_{dl}u(t) \tag{16}$$

with

$$A_{dl} = \begin{bmatrix} 0 & 1 & 0 \\ a_{21} & 0 & a_{23} \\ a_{31} & 0 & a_{33} \end{bmatrix}, B_{dl} = \begin{bmatrix} 0 \\ 0 \\ b_3 \end{bmatrix}$$

$$a_{21} = \frac{x_{30}^2}{m}\frac{F_{emP1}}{F_{emP2}^2}e^{-\frac{x_{10}}{F_{emP2}}}$$

$$a_{23} = -\frac{2x_{30}}{m}\frac{F_{emP1}}{F_{emP2}}e^{-\frac{x_{10}}{F_{emP2}}}$$

$$a_{31} = -(k_iu_0 + c_i - x_{30})\left(\frac{f_{iP1}}{f_{iP2}^2}e^{-\frac{x_{10}}{f_{iP2}}}\right)^2$$

$$a_{33} = -\frac{f_{iP2}}{f_{iP1}}e^{\frac{x_{10}}{f_{iP2}}}$$

$$b_3 = k_i\frac{f_{iP2}}{f_{iP1}}e^{\frac{x_{10}}{f_{iP2}}}.$$

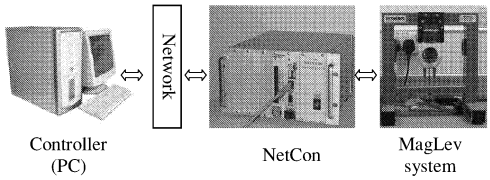

Figure 4. MagLev test rig

Correspondingly, the discrete-time form of (16) with sampling period h is

$$x(k+1) = \Phi_{dl}x(k) + \Gamma_{dl}u(k), \tag{17}$$

where $\Phi_{dl} = e^{A_{dl}h}$ and $\Gamma_{dl} = \int_0^h e^{A_{dl}\eta}d\eta B_{dl}$. Similarly, using a state-feedback control law results in

$$u(k) = K_{dl}\left(x_{ref} - x(k)\right) + u_{ref}. \tag{18}$$

As for the networked predictive control version, recursive calculation of the control prediction sequence similar to (15) can be correspondingly derived.

V. Simulation and Experiments

A. MagLev test rig

The MagLev test rig studied in this paper is set up as shown in Figure 4. The MagLev system is connected to the network via an embedded system – NetCon, and controlled by a remote PC-based controller. This forms a networked control system.

NetCon consists of a main board, an AD/DA board, and a programmable I/O board. The main board has a 32-bit ARM RISC CPU (200MHz), a 64M memory, a network port, etc. NetCon is running on a Linux 2.4-based operating system. More information about NetCon can be found at http://system.research.glam.ac.uk. NetCon is to realize the functions of data acquisition, communication and some other calculation as "smart" actuator or sensor discussed in previous sections. The networked controller runs on a PC (Pentium 2.8GHz) in this test rig, which is programmed using Visual C++. The program includes not only the control law but also the communication with NetCon system to receive the feedbacks of MagLev system and send the control signal. The above test rig can be easily transferred to the local control case by implementing the control law in NetCon system rather than in the PC.

The outputs of the ball position sensor and coil current sensor need to be calibrated to the actual position and current. The results are shown in Table II and III. When the sensed value is not in the table, it is calculated using piece-wise linear interpolation method. Again, this calibration calculation is also done in the "smart" NetCon.

In this paper, the system is set up under an Intranet network. The PC-based controller is with the IP address 192.168.0.12 and NetCon with the address 192.168.0.7. By measuring, the round trip network transmission delay has a maximal 0.02s and there is no data dropout happening in the network. The sampling period $h = 0.01$s is taken, so the round-trip network-induced delay has upper bound $\bar{\tau} = 2$.

Table II
Relation between ball position and sensor output.

ball position (mm)	0	0.7	1.4	2.1	2.8	3.5
sensor output (V)	9.13	9.12	9.12	9.12	9.12	9.11
ball position (mm)	4.2	4.9	5.6	6.3	7	7.7
sensor output (V)	9.10	9.10	9.10	9.09	9.08	9.03
ball position (mm)	8.4	9.1	9.8	10.5	11.2	11.9
sensor output (V)	8.93	8.76	8.52	8.19	7.75	7.2
ball position (mm)	12.6	13.3	14	14.7	15.4	16
sensor output (V)	6.55	5.84	5.15	4.63	4.29	4.11
ball position (mm)	16.8	17.5	18.2	18.9	19.6	20.3
sensor output (V)	4	3.93	3.87	3.83	3.81	3.8

Table III
Relation between coil current and its sensor output.

coil current (A)	2.16	1.95	1.74	1.53	1.32	1.11
sensor output (V)	0.99	1.71	1.62	1.43	1.24	1.04
coil current (A)	0.89	0.67	0.45	0.22	0	
sensor output (V)	0.84	0.63	0.43	0.22	0.04	

The nominal equilibrium point of the ball position is set to 0.01m, and according to (5) the nominal coil current 1.2A and duty cycle 0.4 are obtained. That is to say, $x_{ref} = [0.01\ 0\ 1.2]^T$ and $u_{ref} = 0.4$. In order to reduce violent oscillation of the ball before it becomes stable, a tray is put under the ball to limit the ball position within 0.016m.

B. Simulation

For the feedback linearization method, controller $K_{fl} = [\ 281.77\quad 498.15\quad 21.49\ ]$ is designed for the network-free system (14) with

$$\Phi_{fl} = \begin{bmatrix} 1 & 0.1 & 0.0001 \\ 0 & 1 & 0.01 \\ 0 & 0 & 0 \end{bmatrix}, \Gamma_{fl} = \begin{bmatrix} 0 \\ 0.0001 \\ 0.01 \end{bmatrix}.$$

The system responses for step signal $0.01 \times 1(t)$ are shown in Figure 5, where (a) is for network-free case (local control), (b) is networked control without compensation, and (c) is for networked predictive control. The dash line and solid line represent the reference and the system response, respectively. It can be seen without network-induced delay compensation strategy, K_{fl} can not make the system stable.

For the direct linearization method, at nominal point x_{ref} and u_{ref}, the linearization model is obtained as

$$A_{dl} = \begin{bmatrix} 0 & 1 & 0 \\ 1684.7 & 0 & -19.3 \\ 0 & 0 & -288.8 \end{bmatrix}, B_{dl} = \begin{bmatrix} 0 \\ 0 \\ 726.7 \end{bmatrix}.$$

Further, with sampling period $h = 0.01$, its discrete model is given by

$$\Phi_{dl} = \begin{bmatrix} 1.0854 & 0.0103 & -0.0005 \\ 17.3239 & 1.0854 & -0.066 \\ 0 & 0 & 0.0557 \end{bmatrix}, \Gamma_{dl} = \begin{bmatrix} -0.0013 \\ -0.3324 \\ 2.3763 \end{bmatrix}.$$

The control gain for network-free system is designed as $K_{dl} = [\ -95.6\quad -0.53\quad 0.238\ ]$. To reduce the paper length, the simulation result which is similar to Figure 5 is omitted here.

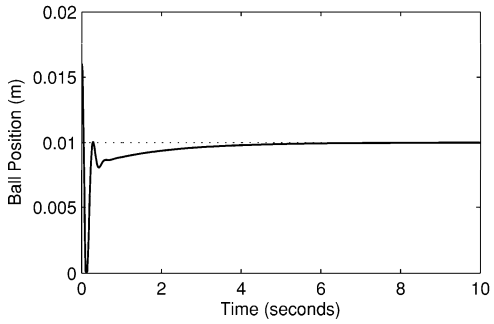

(a) local control

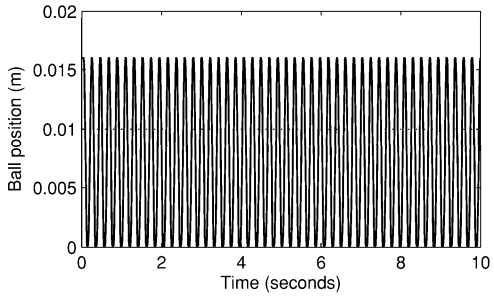

(b) networked control without delay compensation

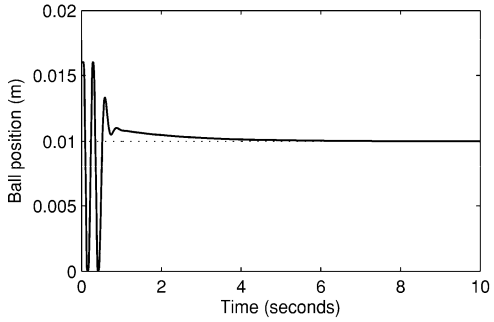

(c) networked predictive control

Figure 5. Simulation of step signal $0.01 \times 1(t)$ tracking of ball position with feedback linearization control.

C. Experiments

In the above methods, the control prediction sequence is very dependent on model accuracy. When the above two predictive control methods are implemented in the real-time system, it is found that neither of them can make the practical system stable. This is because the model is not built very accurately and the MagLev system has the time-varying nature. Thus the result obtain from (16) is not accurate enough to be applied to NPC. It is reasonable to apply on-line model parameter tuning to improve the model accuracy. The feedback linearization method uses the nonlinearization model which is very difficult to tune on-line, so here only the direct linearization method is discussed.

The recursive least square (RLS) method is often used for online parameter estimation and they are adopted here. Expand the state-space model (17) to three separated equations

$$\begin{cases} x_1(k) = & \phi_{11}x_1(k-1) + \phi_{12}x_2(k-1) + \phi_{13}x_3(k-1) \\ & +\gamma_1 u(k-1) \\ x_2(k) = & \phi_{21}x_1(k-1) + \phi_{22}x_2(k-1) + \phi_{23}x_3(k-1) \\ & +\gamma_2 u(k-1) \\ x_3(k) = & \phi_{31}x_1(k-1) + \phi_{32}x_2(k-1) + \phi_{33}x_3(k-1) \\ & +\gamma_3 u(k-1) \end{cases} . \tag{19}$$

For the first equation, it can be rewritten as

$$x_1(k) = \varphi^T(k)\theta,$$

where $\varphi(k) = [x_1(k-1), x_2(k-1), x_3(k-1), u(k-1)]^T$ are past states and control and $\theta = [\phi_{11}, \phi_{12}, \phi_{13}, \gamma_1]^T$ is the parameter vector to be estimated. Thus, the RLS algorithm is obtained as

$$\begin{cases} \hat{\theta}(k) = \hat{\theta}(k-1) + L(k)\hat{\varepsilon}(k) \\ \hat{\varepsilon}(k) = x_1(k) - \varphi^T(k)\hat{\theta}(k-1) \\ L(k) = \dfrac{P(k-1)\varphi(k)}{\lambda + \varphi^T(k)P(k-1)\varphi(k)} \dfrac{\frac{P(k-1)\varphi(k)}{\lambda+\varphi^T(k)P(k-1)\varphi(k)}}{} \\ P(k) = \left(P(k-1) - \dfrac{P(k-1)\varphi(k)\varphi^T(k)P(k-1)}{\lambda(k) + \varphi^T(k)P(k-1)\varphi(k)} \right) / \lambda \end{cases}$$

where λ $(0 < \lambda < 1)$ is called the forgetting factor. Initial $\theta(0)$ can take the value from (17) and $P(0) = \rho I$ with a large ρ. Other parameters in Φ_{dl} and Γ_{dl} can be estimated by a similar procedure using the second and third equations in (19).

In (15), Φ_{dl} and Γ_{dl} should take the estimated values when online parameter estimation is applied. In this case, it can be seen from (19) that not only $x(k)$ but also $x(k-1)$ and $u(k-1)$ should be sent to the remote controller from the MagLev system. Note that because of the network-induced delay, the estimated model $\hat{\Phi}_{dl}(k - \tau_{sc}(k))$ and $\hat{\Gamma}_{dl}(k - \tau_{sc}(k))$ does not reflect the actual system in time, but generally it at least provides an "improved" model. On the other hand, it might be argued that $x(k-1)$ is not necessarily sent with $x(k)$ and $u(k-1)$ because it has already been sent out at $k-1$. This is not true, because the randomness of network-transmission delay or data dropout can not make sure that $x(k - \tau_{sc}(k))$ and $x(k - \tau_{sc}(k) - 1)$ is always available at the same time, which stops the processing of the online estimation algorithm.

The initial values to tune the model are taken from Φ_{dl} and Γ_{dl} calculated in Section V-B. Control results using adaptive networked directive linearization predictive method for set-point response and sine signal tracking of the ball position are shown in Figure 6 and Figure 7 respectively, where the forgetting factor λ takes 0.98 and ρ takes 10000. Figure 6 is the setpoint response for step signal $0.009 + 0.001 \cdot 1(t)$ and Figure 7 is the tracking for the sine signal $0.01 + 0.001 \times \sin(\frac{\pi}{2})$. The dash line and solid line represent the reference and the system response, respectively. These results show the NPC method with on-line model parameter modification is applicable for the real-time implementation of the MagLev system.

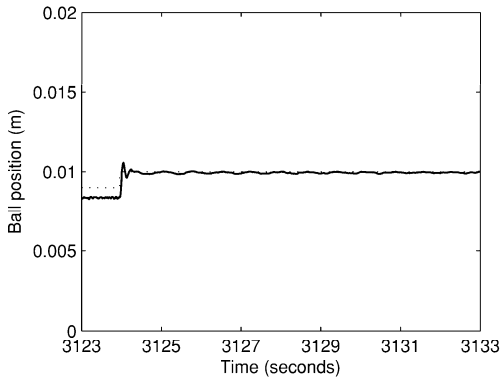

Figure 6. Experiments of setpoint response of ball position 0.01m using adaptive NPC based on direct linearization model

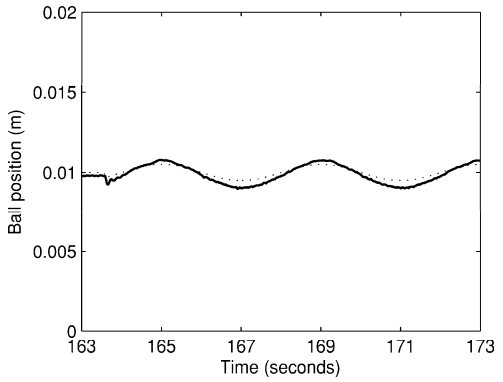

Figure 7. Experiment of sine signal $0.01 + 0.001\sin(\frac{\pi}{2}t)$ tracking of ball position using adaptive NPC based on direct linearization model

VI. Summary

In this paper, the networked control of a magnetic levitation system has been reported. It is about the application of networked predictive control methods. The simulation and experiment results show that these methods are effective for NCSs. The built test rig to implement the above controls can be used as a platform for testing various advanced control algorithms for MagLev system which is typically nonlinear, time-varying and fast, over the network or just using local control.

References

[1] J. R. Downer, "Analysis of single axis magnetic suspension systems," Master's thesis, Dept. Mech. Eng., Massachusetts Inst. Technol., Cambridge, MA, 1980.

[2] N. J. Dahlen, "Magnetic active suspension and isolation," Master's thesis, Dept. Mech. Eng., Massachusetts Inst. Technol., Cambridge, MA, 1985.

[3] M. Dussaux, "The industrial applications of the active magnetic bearings technology," in *Proc. 2nd Int. Symp. Magnetic Bearings*, 1990, pp. 33–38.

[4] D. A. Limbert, H. H. Richardson, and D. N. Wormley, "Controlled characteristics of ferromagnetic vehicle suspension providing simultaneous lift and guidance," *ASME Trans. J. Dyn. Syst. Meas. Control*, vol. 101, pp. 217–222, 1990.

[5] S. Yamamura and H. Yamaguchi, "Electromagnetic levitation system by means of salient-pole type magnets coupled with laminated slotless rails," *IEEE Trans. Vehicular Technol.*, vol. 39, pp. 83–87, 1990.

[6] W. Barie and J. Chiasson, "Linear and nonlinear state-space controllers for magnetic levitation," *Int. J. Syst. Sci.*, vol. 27, no. 11, pp. 1153–1163, 1996.

[7] C. Y. Kim and K. H. Kim, "Gain scheduling control of magnetic suspension systems," in *Proc. Amer. Contr. Conf.*, Jun. 1994, pp. 3127–3131.

[8] A. Charara, J. D. Miras, and B. Caron, "Nonlinear control of a magnetic levitation system without premagnetization," *IEEE Trans. Contr. Syst. Technol.*, vol. 4, pp. 513–523, Sep. 1996.

[9] A. J. Joo and J. H. Seo, "Design and analysis of the nonlinear feedback linearizing control for an electromagnetic suspension system," *IEEE Trans. Contr. Syst. Technol.*, vol. 5, pp. 135–144, Jan. 1997.

[10] D. L. Trumpler, S. M. Olson, and P. K. Subrahmanyan, "Linearizing control of magnetic suspension systems," *IEEE Trans. Contr. Syst. Technol.*, vol. 5, pp. 427–437, Jul. 1997.

[11] A. E. Hajjaji and M. Ouladsine, "Modelling and nonlinear control of magnetic levitation systems," *IEEE Trans. Ind. Electron.*, vol. 48, no. 4, pp. 831–838, Aug. 2001.

[12] D. Cho, Y. Kato, and D. Spilman, "Sliding mode and classical control of magnetic levitation systems," *IEEE Control Syst. Mag.*, pp. 42–48, 1993.

[13] F.-J. Lin, L.-T. Teng, and P.-H. Shieh, "Intelligent adaptive backstepping control system for magnetic levitation apparatus," *IEEE Trans. Magnetics*, vol. 43, no. 5, pp. 2009–2018, May 2007.

[14] Z.-J. Yang, K. Miyazaki, S. Kanae, and K. Wada, "Robust position control of a magnetic levitation system via dynamic surface control technique," *IEEE Trans. Ind. Electron.*, vol. 51, no. 1, pp. 26–34, Feb. 2004.

[15] L. Sun, H. Ohmori, and A. Sano, "Direct closed-loop identification of magnetic suspension system," in *Proc. IEEE Int. Conf. Contr. Appli.*, Hawai, Aug. 1999.

[16] Z.-J. Yang, K. Miyazaki, C.-Z. Jin, and K. Wada, "Physical parameter identification of a magnetic levitation system under a robust nonlinear controller," in *15th Triennial World Congress*, Barcelona, Spain, 2002.

[17] W.-J. Kim, K. Ji, and A. Ambike, "Networked real-time control strategy dealing with stochastic time delays and packet losses," *ASME Trans. J. Dyn. Syst. Meas. Control*, vol. 128, pp. 681–685, Sep. 2006.

[18] ——, "Real-time operating environment for networked control systems," *IEEE Trans. Automat. Sci. Eng.*, vol. 3, no. 3, pp. 287–296, Jul. 2006.

[19] G.-P. Liu, D. Rees, S. Chai, and X. Nie, "Design, simulation and implementation of networked predictive control systems," *Meas. Control*, vol. 38, no. 1, pp. 17–21, Feb. 2005.

[20] G.-P. Liu, Y. Xia, D. Rees, and W. Hu, "Design and stability criteria of networked predictive control systems with random network delay in the feedback channel," *IEEE Trans. Syst., Man, Cybern. C, Appl. Rev.*, vol. 37, no. 2, pp. 173–184, Mar. 2007.

[21] W. Hu, G.-P. Liu, and D. Rees, "Event-driven networked predictive control," *IEEE Trans. Ind. Electron.*, vol. 54, no. 3, pp. 1603–1613, Jun. 2007.

[22] BYTRONIC, *Magnetic levitation system: user's manual*, Bytronic Ltd., 2006.

[23] J. Chiasson, "Ee3648 nonlinear systems class notes," University of Pittsburgh, Pittsburgh, Pensylvania, Tech. Rep., 1989.

[24] A. Isidori, *Nonlinear control systems*. New York: Springer-Verlag, 1989.

[25] H. Nijmeijer and A. V. D. Schaft, *Nonlinear dynamical control systems*. New York: Springer-Verlag, 1990.

[26] W. Zhang, M. S. Branicky, and S. M. Phillips, "Stability of networked control systems," *IEEE Control Syst. Mag.*, vol. 21, no. 1, pp. 84–99, Feb. 2001.

[27] D. Yue, Q.-L. Han, and C. Peng, "State feedback controller design of networked control systems," *IEEE Trans. Circuits Syst. II, Exp. Briefs*, vol. 51, no. 11, pp. 640–644, Nov. 2004.

[28] Y. He, M. Wu, and J.-H. She, "Delay-dependent exponential stability of delayed neural networks with time-varying delay," *IEEE Trans. Circuits Syst. II, Exp. Briefs*, vol. 53, no. 7, pp. 553–557, Jul. 2006.